Received: 9 March 2023 | Revised: 22 November 2023 | Accepted: 27 November 2023

DOI: 10.1111/mmi.15210

RESEARCH ARTICLE

WILEY

Cell death induction facilitates egress of *Coxiella burnetii* from infected host cells at late stages of infection

Jan Schulze-Luehrmann[1] | Elisabeth Liebler-Tenorio[2] | Alfonso Felipe-López[1] | Anja Lührmann[1]

[1]Mikrobiologisches Institut, Universitätsklinikum Erlangen, Friedrich-Alexander-Universität Erlangen-Nürnberg, Erlangen, Germany

[2]Friedrich-Loeffler-Institut, Institut für molekulare Pathogenese, Jena, Germany

Correspondence
Anja Lührmann, Mikrobiologisches Institut – Klinische Mikrobiologie, Immunologie und Hygiene Universitätsklinikum Erlangen, Friedrich-Alexander-Universität Erlangen-Nürnberg, Wasserturmstraße 3/5, Erlangen 91054, Germany.
Email: anja.luehrmann@uk-erlangen.de

Funding information
Bundesministerium für Bildung und Forschung (BMBF), research network zoonotic infectious diseases, Grant/Award Number: 01KI1726A/ 01KI2008A; Deutsche Forschungsgemeinschaft (DFG) through the Priority Programme SPP2225, Grant/Award Number: LU 1357/7-1

Abstract

Intracellular bacteria have evolved mechanisms to invade host cells, establish an intracellular niche that allows survival and replication, produce progeny, and exit the host cell after completion of the replication cycle to infect new target cells. Bacteria exit their host cell by (i) initiation of apoptosis, (ii) lytic cell death, and (iii) exocytosis. While bacterial egress is essential for bacterial spreading and, thus, pathogenesis, we currently lack information about egress mechanisms for the obligate intracellular pathogen *C. burnetii*, the causative agent of the zoonosis Q fever. Here, we demonstrate that *C. burnetii* inhibits host cell apoptosis early during infection, but induces and/or increases apoptosis at later stages of infection. Only at later stages of infection did we observe *C. burnetii* egress, which depends on previously established large bacteria-filled vacuoles and a functional intrinsic apoptotic cascade. The released bacteria are not enclosed by a host cell membrane and can infect and replicate in new target cells. In summary, our data argue that *C. burnetii* egress in a non-synchronous way at late stages of infection. Apoptosis-induction is important for *C. burnetii* egress, but other pathways most likely contribute.

KEYWORDS
apoptosis, *Coxiella burnetii*, egress, Q fever, spreading

1 | INTRODUCTION

Coxiella burnetii is an obligate intracellular Gram-negative pathogen and the causative agent of Q fever, a zoonotic disease with nearly worldwide prevalence (Maurin & Raoult, 1999). Cattle, sheep, and goats are believed to be the main natural reservoir. While an infection is mainly asymptomatic (Angelakis & Raoult, 2010), infected pregnant animals might experience complications, such as abortion, stillbirth, or delivery of weak offspring (Van den Brom et al., 2015). Infected animals shed the pathogen primarily via birthing products, but also via feces and milk into the environment. Humans mainly become infected by inhalation of contaminated aerosols from infected animal livestock (Delsing et al., 2011). The infection is asymptomatic in 60% of the infected humans, while the remaining 40% develop a self-limiting flu-like illness, atypical pneumonia, or hepatitis (Angelakis & Raoult, 2010). In severe cases of acute Q fever, patients can be treated for 14 days with doxycycline (Eldin et al., 2017). However, acute Q fever might lead to fatigue symptoms (Q fever fatigue syndrome—QFS), which might last from a couple of months to several years (Morroy et al., 2016). In rare cases and mainly in patients with predisposing conditions (e.g., cardiac valve anomalies, vascular grafts, and

prosthetic joints), chronic Q fever might develop months or years after the primary infection (Eldin et al., 2017). Chronic Q fever often manifests as endocarditis and *C. burnetii* is found in cardiac valves, the aorta, and in pulmonary arteries, primarily within macrophages and endothelial cells (Maurin & Raoult, 1999). The mortality rate of untreated chronic Q fever can be up to 60%, which can be reduced by antibiotic treatment to less than 5%. However, patients have to be treated with doxycycline in combination with chloroquine for at least 18–24 months (Anderson et al., 2013). This long treatment may be accompanied by severe side effects such as photosensitization, food intolerance, retinal toxicity or irreversible skin pigmentation (Kersh, 2013) and, as a consequence, to reduced compliance.

Alveolar macrophages are the first cells to encounter the pathogen (Maurin & Raoult, 1999). However, during the course of infection, *C. burnetii* infects other cell types, including endothelial cells, fibroblasts, trophoblasts and epithelial cells. Bacterial uptake was shown to be mediated by $\alpha_v\beta_3$ integrins (Capo et al., 1999) or the *C. burnetii* encoding invasin OmpA (Martinez et al., 2014). The bacteria remain in a vacuole, called the *C. burnetii*-containing vacuole (CCV) (Dellacasagrande et al., 2000; Martinez et al., 2014). The CCV matures along the default endocytic pathway from early endosomal to phagolysosomal stages (Howe et al., 2010; Voth & Heinzen, 2007). The only differences to the canonical phagosome maturation process are the interactions with autophagosomes as early as 5 min after uptake and with secretory vesicles at later stages (Campoy et al., 2011; Gutierrez et al., 2005; Schulze-Luehrmann et al., 2016). The pH within the CCV drops to 4.5, which triggers expression and activity of the type IVB secretion system (T4BSS) (Newton et al., 2013). The T4BSS is essential for *C. burnetii* intracellular replication and translocates bacterial virulence factors, so-called effector proteins, into the host cell cytoplasm (Beare, Gilk, et al., 2011; Carey et al., 2011), where they manipulate host cell processes. To date, around 150 effector proteins are known. However, a function has only been assigned to a part of them (Larson et al., 2016; Lührmann et al., 2017). The effector proteins CvpA, Cig57, and CirA manipulate intracellular trafficking events (Larson et al., 2013, 2015; Latomanski et al., 2016; Weber et al., 2016), while CvpB facilitates the association of CCVs with autophagosomes (Kohler et al., 2016; Martinez et al., 2016). Five effector proteins (MceA-E) associated with mitochondria (Fielden et al., 2017, 2021), and a few effector proteins (CBU0129, CBU0388, CBU0393, AnkG, CBU0794, CBU0937, NopA, CBU1314, CaeA, and CBU1976) have nuclear localization (Burette et al., 2020; Carey et al., 2011; Chen et al., 2010; Cordsmeier et al., 2022; Schäfer et al., 2017; Weber et al., 2013). In addition, four effector proteins (AnkG, CaeA, CaeB, and IcaA) have been identified to inhibit host cell apoptosis (Bisle et al., 2016; Cordsmeier et al., 2022; Eckart et al., 2014; Klingenbeck et al., 2013; Lührmann et al., 2010; Schäfer et al., 2017, 2020), or pyroptosis (Cunha et al., 2015). Manipulation of vesicular trafficking and inhibition of apoptosis are essential virulence mechanisms that permit intracellular replication of *C. burnetii* (Lührmann et al., 2017). The bacteria multiply until the mature CCV occupies most of the host cell cytoplasm (Howe et al., 2003). Importantly, while we have information about the initial step of *C. burnetii* uptake and the maturation process of the CCV, it is completely unknown how *C. burnetii* spreads, that is, how it exits its host cell to enter new target cells (Coleman et al., 2004). Understanding this essential step will be crucial to develop novel strategies to prevent *C. burnetii* from spreading and, thus, disease.

2 | RESULTS

2.1 | *C. burnetii* controls host cell apoptosis in a temporal manner

C. burnetii replicates to high numbers within the CCV, without obvious negative impact on cell viability (Baca et al., 1985) and no synchronized egress event (Larson et al., 2016). Nevertheless, it was hypothesized that induction of apoptosis might facilitate the spreading of the infection to nearby susceptible cells (van Schaik et al., 2013). So far, the majority of reports demonstrate that *C. burnetii* possesses anti-apoptotic activity (Cordsmeier et al., 2019; Lührmann & Roy, 2007; Voth et al., 2007). However, there are also a few publications showing that *C. burnetii* induces apoptosis (Zhang et al., 2012). Importantly, several pathogens have the ability to both inhibit and activate host cell death in a temporally controlled manner (Friedrich et al., 2017).

Therefore, we aimed to determine how *C. burnetii* influences host cell apoptosis during the course of infection. We measured apoptosis by Annexin V staining using flow cytometry and by assaying the cleavage of poly ADP-ribose polymerase (PARP) by immunoblot, the latter as a marker for the terminal stages of apoptosis. Importantly, ~70% of cells were infected at day 2 and 7 post-infection. We determined the percentage of Annexin V-positive cells only from infected cells (gated for cells infected with GFP-expressing *C. burnetii*), while PARP cleavage was determined from all cells in the culture.

At 2 days post-infection, *C. burnetii* did not induce apoptosis but inhibited staurosporine-induced apoptosis (Figure 1a). Thus, while ~27% of uninfected cells were Annexin V positive after staurosporine treatment, this was reduced to ~13% by infection with *C. burnetii*. In contrast, at 7 days post-infection we observed induction of apoptosis, even without staurosporine treatment. Thus, 3% of the uninfected cells were Annexin V positive, while the infection for 7 days increased this rate to 21%. Furthermore, at this late time point of infection, *C. burnetii* did not inhibit but instead boosted staurosporine-induced apoptosis. Thus, ~44% of infected cells were Annexin V positive, while only ~27% of uninfected cells were Annexin V positive (Figure 1a,b). Similar results were obtained by analyzing the cleavage of PARP (Figure 1c). These data indicate that *C. burnetii* inhibits host cell apoptosis at early time points of infection while inducing or boosting this form of programmed cell death at later stages of infection.

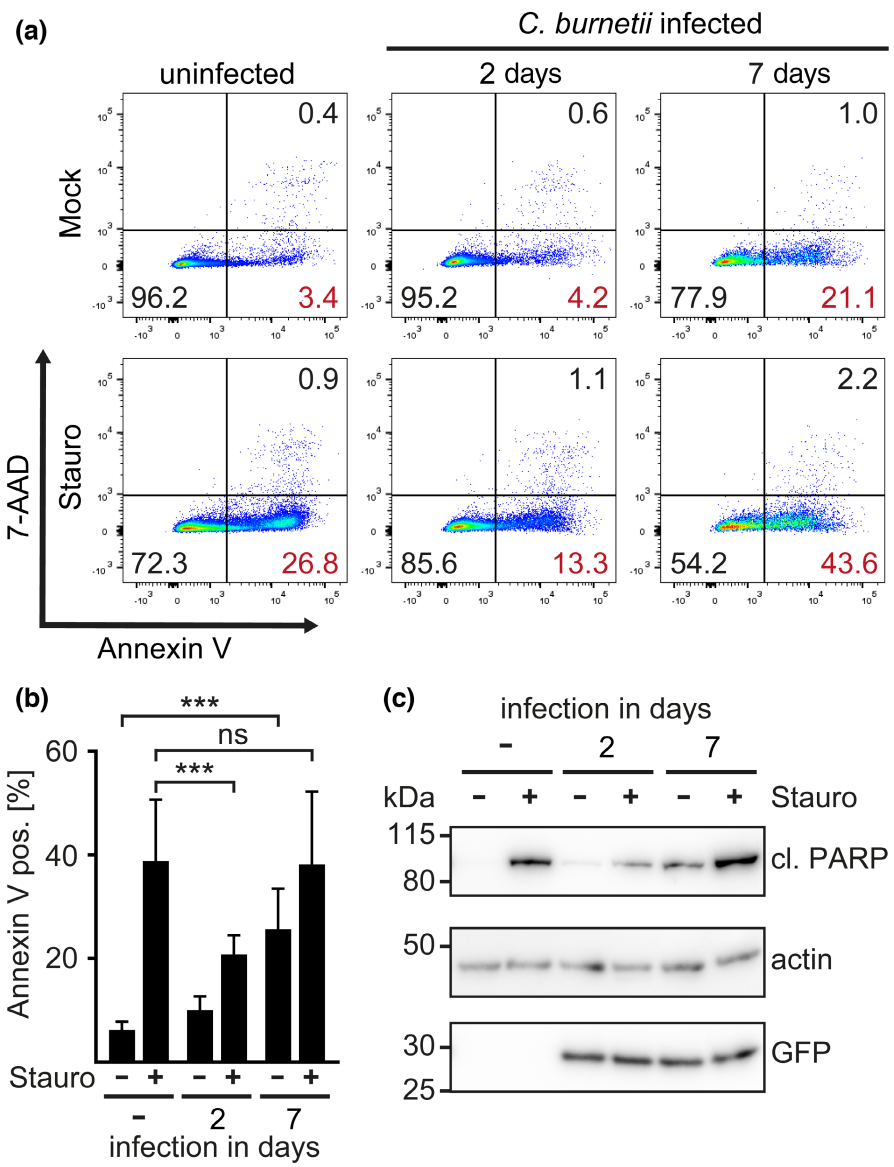

FIGURE 1 *Coxiella burnetii* inhibits apoptosis early, but boosts apoptosis late during infection. HeLa cells, either uninfected or infected with GFP-tagged *C. burnetii* for 2 or 7 days were either not treated or treated with staurosporine for 4 h. (a) Cells were stained with Annexin V-PE and 7-AAD. Apoptosis was determined by FACS measurement as PE-positive and 7-AAD-negative cells. For the *C. burnetii* infected samples shown data were gated on the GFP-positive population. One representative data set is shown (b) Quantification of Annexin V-positive and 7-AAD-negative cells in percent from three independent experiments. (c) Protein lysates were separated by SDS-PAGE, transferred to a PVDF membrane, and probed with anti-cleaved PARP antibody to visualize cell death, anti-actin as protein loading control, and anti-GFP to demonstrate *C. burnetii* infection. Depicted is one representative experiment out of three independent experiments with similar results. ns > 0.05, ***$p < 0.001$.

2.2 | *C. burnetii* egresses from infected cells at late stages of infection

Bacteria exploit different pathways to exit their host cell. These include (i) initiation of programmed cell death, (ii) active destruction of the host cell, and (iii) exocytosis of membrane-bound vesicles without host cell lysis (Flieger et al., 2018). To get a first impression of the ability of *C. burnetii* to egress from infected cells, we performed live cell imaging of SiR actin-labeled human endothelial cells (EA.hy926) infected with mCherry-expressing *C. burnetii*. We used EA.hy926 cells as *C. burnetii* replicate to high numbers in this cell type, and we reasoned that this might help to investigate egress mechanisms. In addition, endothelial cells are also target cells of *C. burnetii* during in vivo infection (Atzpodien et al., 1994). Furthermore, we concentrated on the later stages of infection, as we hypothesized that egress might correlate with *C. burnetii*-induced host cell apoptosis (Figure 1). We detected release of bacteria (Figure 2a, arrowheads) and potential apoptotic bodies (Figure 2a, asterisks) 5 days post-infection. In addition, we observed fission events of the CCV (Figure 2b, arrowheads) and egress of *C. burnetii* without cell death (Figure 2b, square). This indicates that *C. burnetii* might be able to egress infected cells and that apoptosis is not necessarily associated with this process. Furthermore, it results in several open questions regarding the role of cell death-dependent versus independent processes in egress, the role and importance of CCV fission in egress and the infectivity of egressed bacteria.

To address the latter, we performed a co-culture experiment. CFSE-labeled uninfected cells were co-cultured with unlabeled cells infected for 5 days with TagRFP-expressing *C. burnetii* (Figure 3a, open arrowhead). *C. burnetii* were detected in the previously uninfected CFSE-labeled cells at 24 h co-culture (Figure 3a, filled arrowheads). The establishment of spacious CCVs was observed at 48 h co-culture (Figure 3a, filled arrowheads), indicating that the egressed bacteria are able to infect and replicate within the new host cells. To minimize the possibility that extracellular instead of prior intracellular bacteria account for the infection of prior uninfected cells, we aimed to kill extracellular *C. burnetii*. A high concentration of 200 μg/mL

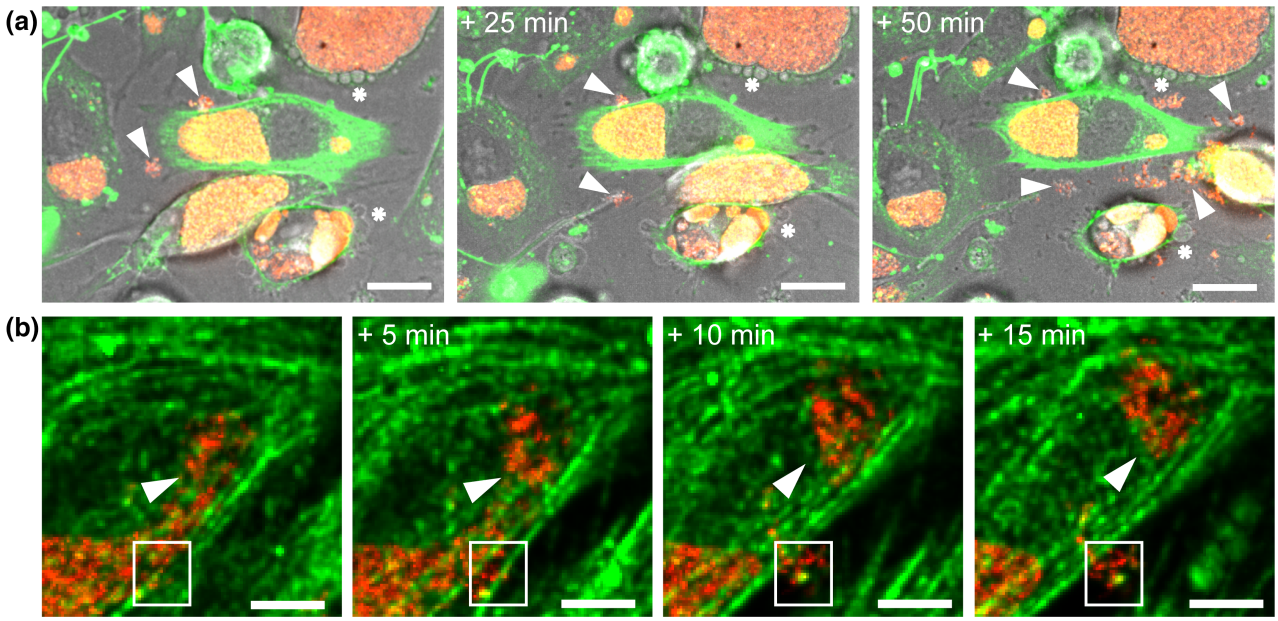

FIGURE 2 *Coxiella burnetii* mCherry escapes from endothelial EA.hy926 cells. EA.hy926 cells infected with *C. burnetii* mCherry (red), were stained with SiR-actin (green) and imaged 5 days post-infection with a Zeiss spinning disk Z1 confocal laser scanning microscope. (a) 5 h post-imaging, infected cells were monitored every 25 min over a 50-minute period. Asterisks mark potential apoptotic bodies and arrowheads point to egressed *C. burnetii*. Scale bar represents 20 μM. (b) 3 h post-imaging an infected cell was monitored every 5 min over a 15-minute period. The arrowhead points out a fission process of a CCV. The egress of *C. burnetii* is shown in the square. Scale bare represent 15 μM.

gentamicin eliminates over 80% of *C. burnetii* (Figure 3b). Even under these conditions, we detected spreading of infection to prior uninfected cells. At 24 h co-culture ~30% of the prior uninfected cells were infected. This rate increased over the time of co-culture, reaching ~80% at 72 h (Figure 3c).

2.3 | Cell-to-cell contact is not needed for spreading of *C. burnetii*

While our data (Figures 2 and 3) suggest that the bacteria are released and spreading does not happen via membrane protrusions (Weddle & Agaisse, 2018), we performed a trans-well assay to challenge this assumption. Thus, CFSE-labeled uninfected EA.hy926 cells were seeded at the bottom of a trans-well plate. Cells infected with TagRFP-labeled *C. burnetii* were placed in the upper well. The pore size of 3 μm prevents cells from the upper well from reaching the lower well. Starting from 24 h co-culture, we observed infected cells in the lower well (Figure 4a). The fraction of infected cells in the lower chamber increased as well as the size of the CCVs over the incubation time. Thus, the percentage of infected cells in the lower chamber increased from ~20% at 24 h of culture to ~90% at 96 h of culture (Figure 4b). These data indicate that *C. burnetii* spreading does not require cell-to-cell contact.

2.4 | Egress depends upon bacterial load

C. burnetii spreading was time-dependent (Figures 3c and 4b), but the underlying reason is unknown. As *C. burnetii* egress does not appear to be synchronized, we hypothesized that egress might be triggered by the physiologic condition/metabolic status within the individual infected cell. Thus, a lack of available host cell nutrients, which can be the consequence of bacterial replication and/or number, might induce egress from an individual infected cell. To quantify the ability of *C. burnetii* to spread to prior uninfected cells, we established a FACS-based spreading assay (Figure S1). Indeed, the multiplicity of infection (MOI) affects spreading ability (Figure 5a). While a MOI of 2 did not induce bacterial spreading over the time period of the experiment (96 h), a MOI of 200 did. This suggests that a high bacterial load is required for bacterial egress. An infection with a MOI of 2 and 20 only resulted in small CCVs at 7 days post-infection, which increased within the next 2 days (Figure 5b). Importantly, a MOI of 50 or 200 resulted in large CCVs at 7 days post-infection. Within the next 2 days of infection, the large CCVs seemed to disintegrate, forming several small CCVs (Figure 5b). This phenotype seems to be associated with the release of bacteria and spreading of the infection.

2.5 | Released *C. burnetii* are not covered by a host cell membrane

Our data suggests that *C. burnetii* are released from infected cells. However, it is unclear whether the pathogen is covered by a host cell membrane or not. To analyze this, we first asked whether gentamicin treatment affects spreading of *C. burnetii*. Gentamicin kills extracellular, but not intracellular bacteria, as it only poorly penetrates eukaryotic cells. As the high gentamicin concentrations

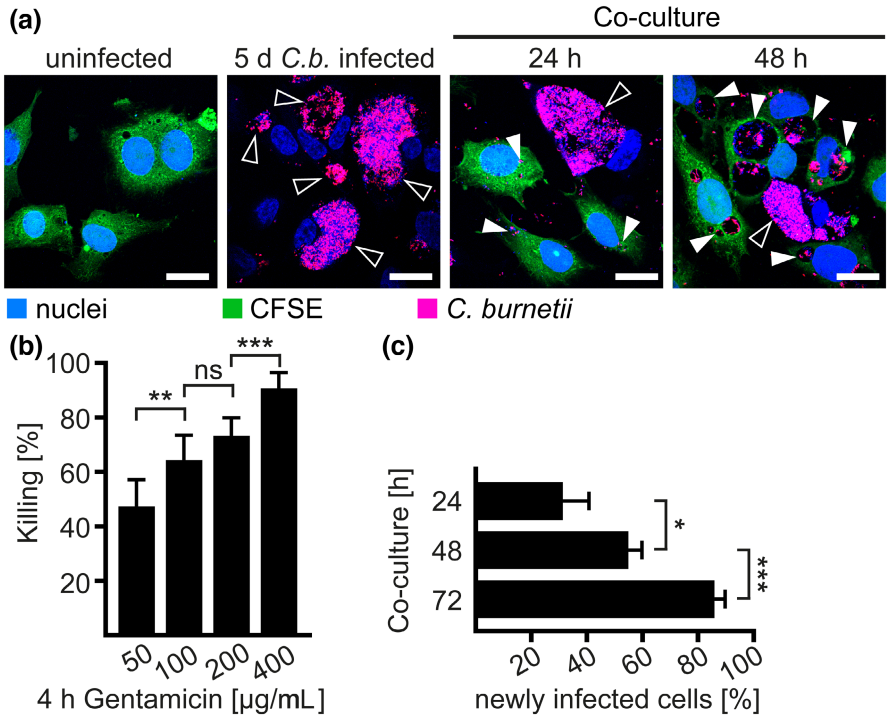

FIGURE 3 *Coxiella burnetii* spread from infected to uninfected endothelial EA.hy926 cells in co-culture. (a) Uninfected EA.hy926 cells stained with CFSE (green) and EA.hy926 cells infected with *C. burnetii* TagRFP (magenta) for 5 days at a MOI of 200 were co-cultivated at a ratio of 2:1 and visualized 24 h and 48 h later with a Zeiss confocal laser scanning microscope LSM700. DNA is stained by DAPI (blue). Empty arrowheads point to *C. burnetii*-containing vacuoles (CCVs) in infected cells and filled arrowheads point to CCVs of prior uninfected CFSE-labeled cells. Scale bar equals 20 µM. (b) *C. burnetii* were incubated for 4 h with the indicated concentrations of gentamicin and then transferred into ACCM-2 axenic growth medium. After 3 days at 37°C, 5% CO_2, and 2.5% O_2, the OD_{600} was measured and percent killing in comparison to untreated bacteria calculated. Plotted are the mean percentage and standard deviation of three independent experiments in duplicate. ns > 0.05, $^{**}p < 0.01$, $^{***}p < 0.001$. (c) Uninfected EA.hy926 cells were stained with CFSE. EA.hy926 cells were infected with *C. burnetii* TagRFP at a MOI of 200 and cultured for 5 days. Infected cells were treated with 200 µg/mL gentamicin for 4 h. Uninfected and infected cells were co-cultivated at a ratio of 2:1. At 24, 48, and 72 h, the percentage of newly infected CFSE-labeled cells was determined using a Zeiss confocal laser scanning microscope LSM700. Shown are the mean percentage and standard deviation of three independent experiments. ns > 0.05, $^{*}p < 0.05$, $^{**}p < 0.01$, $^{***}p < 0.001$.

required for killing of ~80% of the bacterial population might also impact intracellular bacteria (VanCleave et al., 2017), we determined the ability of *C. burnetii* to replicate intracellularly in the presence of gentamicin in the medium. Treatment of infected cells with 200 µg/mL gentamicin over a period of 2 or 5 days did not influence bacterial replication, as demonstrated by immunofluorescence microscopy and CFU counts (Figure 6a,b). Importantly, spreading of *C. burnetii* to uninfected cells was significantly inhibited by gentamicin treatment (Figure 6c). These data suggest that the *C. burnetii* released are susceptible to gentamicin and, thus, probably not covered by a host cell membrane. To verify this assumption, we performed electron microscopy of infected cells and of released *C. burnetii* in the cell supernatant. First, we analyzed *C. burnetii*-infected EA.hy926 cells at 7 days post-infection. As shown in Figure 7a, we observed cells filled with large CCVs (marked with 1 and 2), but also a lysed cell with cytoplasm (marked with C), loss of organelles, fragmented plasma membrane (marked with arrows) and shrunken pyknotic nuclei with condensed chromatin (marked with N). *C. burnetii* was found in the lytic cytoplasm (marked with 3). Figure 7b, a magnification of the region marked in Figure 7a, showed that the bacteria were not surrounded by a host cell membrane. These images indicate that cell death, either apoptotic or lytic, might be involved in *C. burnetii* egress.

Next, we collected the supernatant of cells infected for 10 days with *C. burnetii*. We detected nuclei with condensed chromatin (marked with N), which might be a sign of apoptosis, and accumulations of *C. burnetii* (marked with 1, 2, and 3), which might represent former CCVs (Figure 7c,e). By magnification of the dotted squares (Figure 7d,f), we were able to demonstrate that these accumulations of bacteria were not surrounded by a membrane and contained cell debris (marked with D). In addition, the bacterial accumulations were composed of large cell variants (LCV, marked with white arrows) and only a few small cell variants (SCV, marked with black arrows), which are two pleomorphic forms of *C. burnetii*. SCVs are characterized by their 0.2 to 0.5 µm long rod-shaped structure with electron-dense nucleoids and a thick cell wall. They represent the non-replicating, metabolically inactive, but environmentally stable form of *C. burnetii*. LCVs are the up to 2 µm long replicative forms of *C. burnetii*, are themselves pleomorphic, and have dispersed chromatin (Maurin & Raoult, 1999; Moormeier et al., 2019). Together, these data support

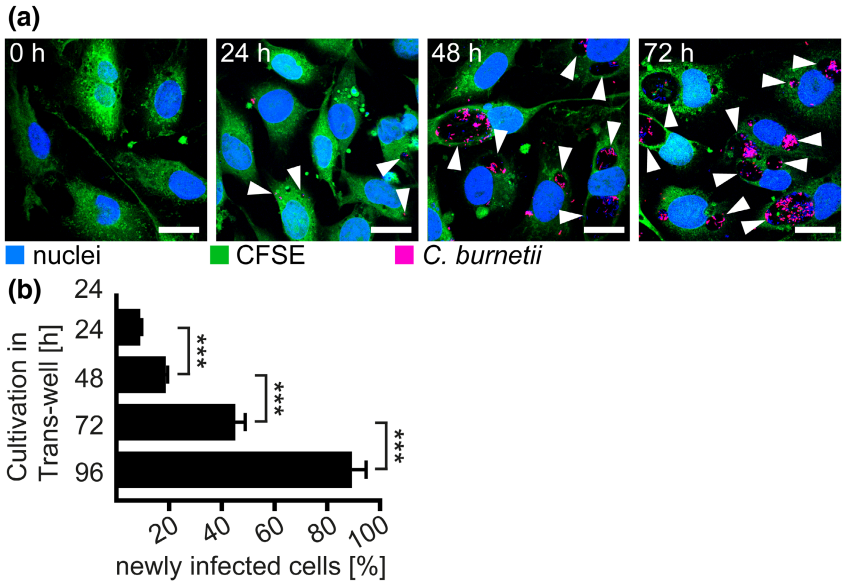

FIGURE 4 Spreading of *Coxiella burnetii* does not require cell-to-cell contact. (a) EA.hy926 cells were infected with *C. burnetii* TagRFP (magenta) at an MOI 200 and cultured for 5 days in the upper chamber of a trans-well system with 3 μm pore size. CFSE-labeled uninfected EA.hy926 cells (green) were placed in the lower chamber for the indicated time periods. DNA is stained with DAPI (blue). Shown are representative images of the lower chamber taken by a Zeiss confocal laser scanning microscope LSM700. Filled arrowheads point to *C. burnetii*-containing vacuoles. The scale bar is 20 μM. (b) EA.hy926 cells were infected with *C. burnetii* TagRFP at a MOI 200 and cultured for 5 days in the upper chamber of a trans-well system with 3 μm pore size. Infected cells were treated with 200 μg/mL gentamicin for 4 h. CFSE-labeled uninfected EA.hy926 cells were placed in the lower chamber. At 24, 48, 72, and 96 h, the percentage of infected CFSE-labeled cells was determined using a Zeiss confocal laser scanning microscope LSM700. Shown are the mean percentage and standard deviation of three independent experiments. $^{***}p < 0.001$.

our previous results and confirm that released bacteria are not covered by a host cell membrane. In addition, these data indicate that bacterial egress might be associated with host cell death.

2.6 | Intrinsic apoptosis induction facilitates *C. burnetii* spreading

Several pathogens induce programmed cell death pathways to egress from the host cells (Flieger et al., 2018). It was suggested for *C. burnetii*, that host cell apoptosis might be important for spreading (van Schaik et al., 2013). In addition, our data also suggest that apoptosis might be associated with *C. burnetii* egress (Figures 2a and 7a,c). To investigate the role of apoptosis in *C. burnetii* egress, we employed HeLa cells either lacking the pro-apoptotic Bax/Bak proteins or overexpressing the anti-apoptotic Bcl_{XL} protein. The deletion of Bax and Bak, as well as the overexpression of Bcl_{XL}, block the intrinsic apoptosis pathway (Brokatzky et al., 2019, 2020). Importantly, spreading was reduced in both cell lines compared to the two parental HeLa cell lines (Figure 8a,b). However, spreading was not completely abolished, indicating that apoptosis is involved in *C. burnetii* egress and spreading, but that other pathways, such as lytic cell death or exocytosis, might also contribute.

Previous reports indicated that *C. burnetii* inhibits cell death of its host cell (Cordsmeier et al., 2019; Cunha et al., 2015; Lührmann & Roy, 2007; Voth et al., 2007). In addition, anti-apoptotic T4BSS effector proteins have been identified (Bisle et al., 2016; Cordsmeier et al., 2022; Cunha et al., 2015; Eckart et al., 2014; Klingenbeck et al., 2013; Lührmann et al., 2010; Schäfer et al., 2017, 2020). As we observed possible apoptotic bodies in the proximity of egressed *C. burnetii* (Figure 2a), induction of the intrinsic apoptotic pathway might be involved in *C. burnetii* spreading (Figure 8). Indeed, at late stages of infection, infected HeLa cells showed signs of apoptosis and were not protected from staurosporine-induced intrinsic apoptosis (Figure 1a–c). Similarly, we observed fragmented nuclei in staurosporine-treated HeLa cells infected with *C. burnetii* for 5 days. This resulted in reduced size of CCVs (Figure 9a,b). In contrast, staurosporine treatment of HeLa cells either overproducing Bcl_{XL} or lacking Bax and Bak showed no signs of fragmented nuclei and contained large CCVs (Figure 9a,b). This supports our results that at late stages of infection, *C. burnetii* is unable to protect its host cell from apoptosis induction. Importantly, in the supernatant of HeLa cells infected for 5 days, we detected significant numbers of viable *C. burnetii*, as measured by CFU (Figure 9c). In contrast, in the supernatant of HeLa cells either overproducing Bcl_{XL} or lacking Bax and Bak, only very few bacteria were found (Figure 9c), indicating that in the absence of a functional intrinsic apoptosis pathway, *C. burnetii* egress is hampered. This is further supported by increased number of bacteria in the supernatant of staurosporine-treated cells (Figure 9c). Together these data indicate that apoptosis is involved in *C. burnetii* egress. However, our data also suggest that other pathways are also important for *C. burnetii* egress.

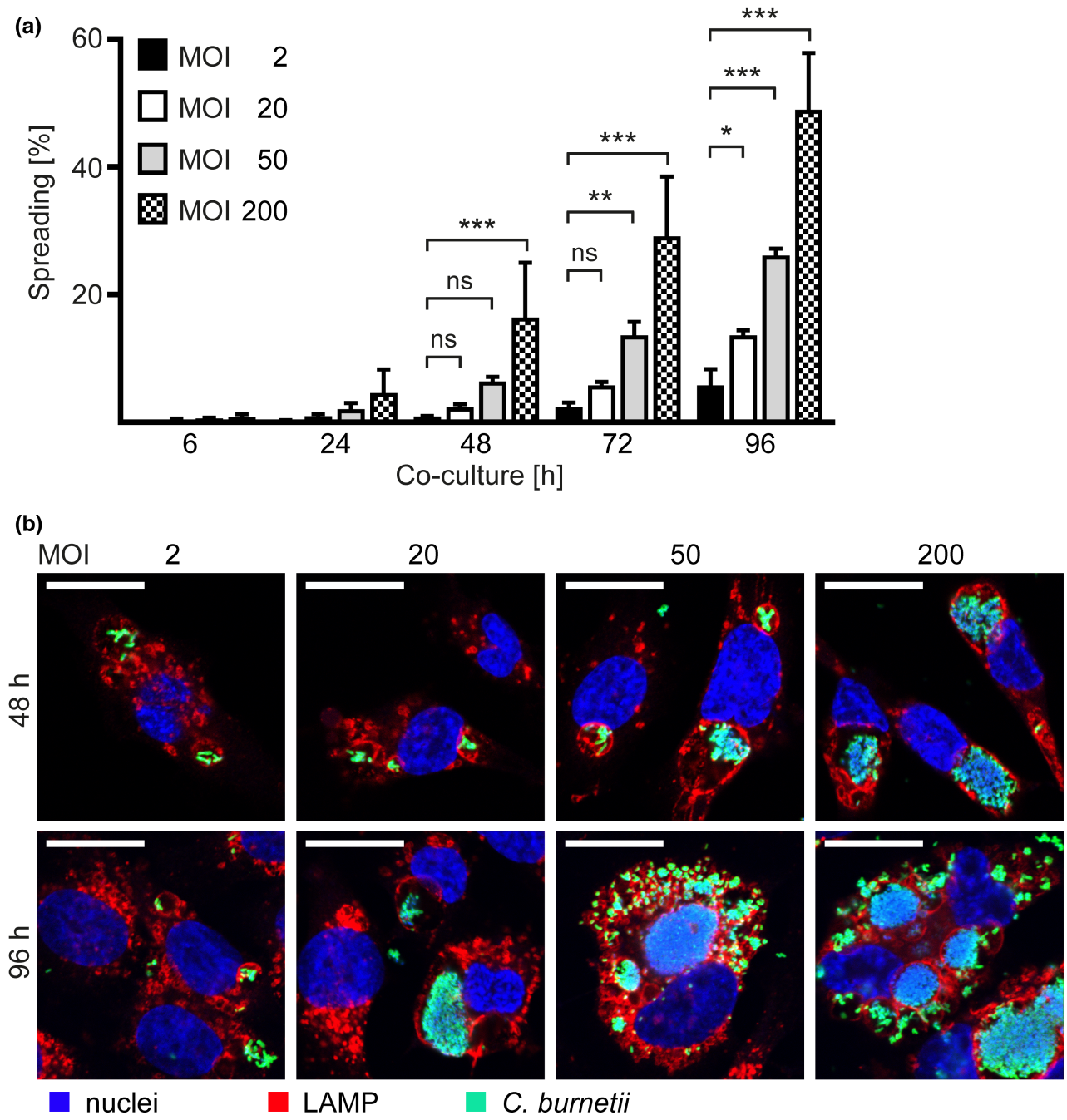

FIGURE 5 Spreading of infection is influenced by CCV size. (a) Uninfected EA.hy926 cells were labeled with CellTrace Blue. EA.hy926 cells were infected with *C. burnetii* GFP at the indicated MOIs. After 5 days, the infected cells were incubated with 200 μg/mL gentamicin for 4 h. The cells were incubated together at a ratio of 1:2 (infected: uninfected) for the indicated time periods. 30.000 single cells were analyzed by flow cytometry (BD LSRFortessa) for each sample. Data represent mean percentage ± SD of GFP- and CTB-positive cells out of total CTB-positive cells from three independent experiments in duplicate. ns > 0.05, $^{*}p < 0.05$, $^{**}p < 0.01$, $^{***}p < 0.001$. (b) EA.hy926 cells after 5 days of infection with *C. burnetii* GFP at the indicated MOIs were seeded on coverslips for 48 or 96 h, fixed and stained for LAMP-1 (red), for *C. burnetii* (green) and for DNA (blue). Shown are representative images from three independent experiments. Each Scale bar is 20 μM.

3 | DISCUSSION

Adaption of intracellular pathogens to their host cell is particularly relevant for obligate intracellular bacteria, as they require their host cell for survival and replication. The pathogen–host interaction is complex. Pathogens have to invade, survive the host intrinsic defense mechanisms, establish their replicative niche, and eventually leave the host cell to spread within the tissue or the whole organism. The latter event is critical for pathogen dissemination but is not well studied for several pathogens, including the obligate intracellular pathogen *C. burnetii*. The mode of *C. burnetii* egress is unknown (Coleman et al., 2004). However, it has been suggested that

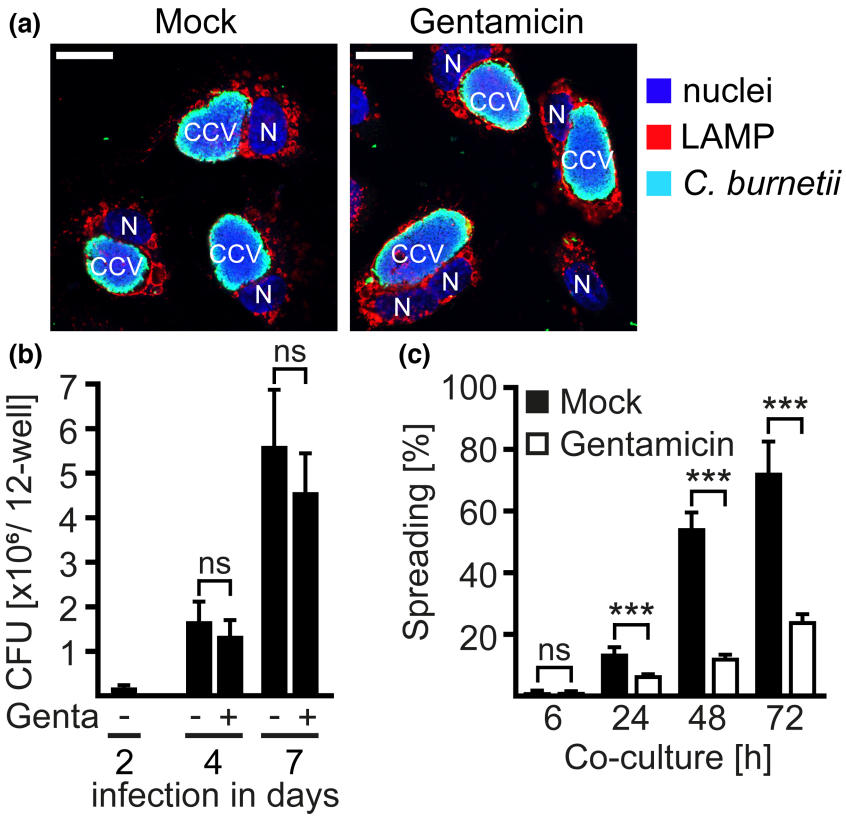

FIGURE 6 *Coxiella burnetii* spreading is inhibited by gentamicin treatment. Cells were infected for 5 days (a, c) or 2 days (b) with GFP-tagged *C. burnetii* at MOI 200. Cells were further incubated without (Mock) or with 200 μg/mL gentamicin for the indicated time periods. (a) The cells were fixed after 72 h treatment and stained for LAMP-1 (red), *C. burnetii* (green), and DNA (blue). Shown are representative images from three independent experiments. Each scale bar represents 20 μM. (b) The cells were lysed at the indicated time points post-infection by incubation in ice-cold ddH_2O and repeated pipetting. The lysates were plated as triplicates onto ACCM-D agar plates in 10-fold dilution. The plates were incubated for 10 days and colony-forming units were counted. Unpaired t-test, $n = 3$. ns > 0.05, ***$p < 0.001$. (c) EA.hy926 cells were infected with *C. burnetii* GFP at MOI 200. After 5 days of infection, cells were incubated with 200 μg/mL gentamicin for 4 h to kill extracellular *C. burnetii*. Uninfected EA.hy926 cells were labeled with CellTrace Blue (CTB). Infected and uninfected cells were cultivated together at a ratio of 1:2 (infected: uninfected) for the indicated time periods indicated and 30.000 single cells were analyzed by flow cytometry (BD LSRFortessa) for each sample. Shown are the mean percentage of GFP- and CTB-positive cells out of total CTB-positive cells from three independent experiments in duplicate. Error bars indicate mean ± SD, ns > 0.05, ***$p < 0.001$.

apoptosis-induction might enable spreading of the infection (van Schaik et al., 2013). Here we demonstrated that *C. burnetii* egresses from its host cell at late stages of infection (Figure 2) and spreads to new target cells (Figures 3 and 4). As *C. burnetii* egress depends upon high bacterial load (Figure 5), one may speculate that limitation of metabolites or essential nutrients might be physiological cues to trigger bacterial egress. Thus, iron limitation triggers egress of the evolutionarily related intracellular pathogen *Legionella pneumophila* (O'Connor et al., 2016). Whether iron limitation also triggers *C. burnetii* egress has to be determined, as conflicting roles for iron in *C. burnetii* pathogenesis have been reported (Briggs et al., 2008; Howe & Mallavia, 1999; Sanchez & Omsland, 2020). Since *C. burnetii* is auxotroph for 11 amino acids (Sandoz et al., 2016), amino acid limitation might also be a possible trigger of egress. While the trigger(s) of *C. burnetii* egress is still unknown, we started to elucidate the mode of egress, since intracellular bacteria can use different ways to exit the host cell. This includes induced programmed host cell death, active host cell destruction, and membrane-dependent exit without host cell destruction (Flieger et al., 2018; Friedrich et al., 2012). We observed the presence of potential apoptotic bodies in proximity to egressed *C. burnetii* (Figure 2) and identified the ability to undergo intrinsic apoptosis as important for bacterial spreading (Figures 1, 8, and 9), indicating that apoptosis-induction is involved in *C. burnetii* egress. Whether apoptosis is the only cell death pathway involved in *C. burnetii* egress has to be determined. Indeed, the morphology of dead cells (Figure 7a) suggests that lytic forms of programmed cell death, for example, pyroptosis or necroptosis, might additionally be associated with egress and interaction between different forms of programmed cell death pathways has been described (Bertheloot et al., 2021). Several successful intracellular pathogens suppress cell death during the replicative phase but induce cell death to egress and disseminate (Friedrich et al., 2012; Koch et al., 2020; Traven & Naderer, 2014). This also seems to be true for *C. burnetii* (Figure 1a–c). The T4BSS has been shown to be essential for modulation of host cell apoptosis (Beare, Gilk, et al., 2011). Indeed, anti-apoptotic T4BSS effector proteins have been identified (Beare, Gilk, et al., 2011;

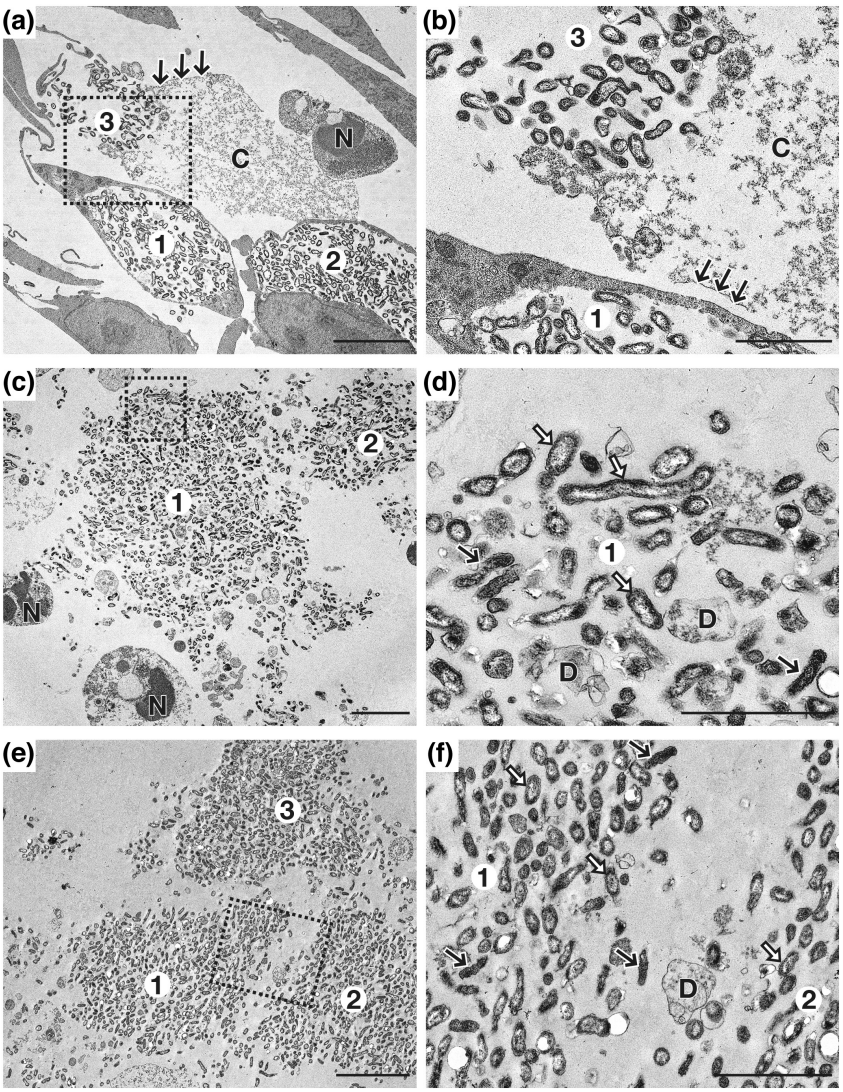

FIGURE 7 Egressed *Coxiella burnetii* is not covered by a host cell membrane. (a, b) EA.hy926 cells were infected with *C. burnetii* for 7 days. Cells were prepared for transmission electron microscopy. Ultrathin sections of infected cells are shown. (a) Two cells with large CCVs (1 and 2) and one cell with shrunken, pyknotic nucleus with condensed chromatin (n), lytic cytoplasm (c), fragmented plasma membrane (remnants indicated by arrows), and accumulations of *C. burnetii* (3) are shown. Scale bar = 5 μm. (b) Higher magnification of a part of (a), indicated by dotted lines. In contrast to *C. burnetii* in the CCV of the intact cell (1), *C. burnetii* in the disintegrated cell (3) are free in the extracellular space and not engulfed by a host cell membrane. Scale bar = 2 μm. (c–f) EA.hy926 cells were infected with *C. burnetii* for 10 days. The supernatants were collected and centrifuged. The pellets were prepared for transmission electron microscopy. Ultrathin sections of pelleted supernatant are shown. (c, e) Accumulations of *C. burnetii* (1, 2, 3) and pyknotic nuclei with condensed chromatin (N) are shown. Scale bar = 5 μm. (d, e) Higher magnification of a part of (c, e), indicated by dotted lines. Accumulations of *C. burnetii* (1) consisting of LCV (open arrows) and SCV (black arrows) and cell debris (d) are not surrounded by host cell membranes. Scale bar = 2 μm.

Bisle et al., 2016; Cordsmeier et al., 2022; Klingenbeck et al., 2013; Lührmann et al., 2010; Lührmann & Roy, 2007; Voth et al., 2007; Voth & Heinzen, 2009), and potential cell death-triggering or -enhancing effector proteins might exist (Klingenbeck et al., 2013; Martinez et al., 2014). This opens the possibility that T4BSS effector proteins might be required for *C. burnetii* egress. Further research is required to dissect the role of the T4BSS in egress and spreading of *C. burnetii* and identify potential effector proteins involved in these processes.

We noticed that cell-to-cell contact is not needed for bacterial spreading (Figure 4) and that egressed bacteria are not surrounded by a host cell membrane (Figure 7), which is in line with the fact that egressed bacteria are susceptible to gentamicin treatment (Figure 6c). The majority of the egressed bacteria seem to be LCV (Figure 7d,f), which is the metabolically more active and replicative form (van Schaik et al., 2013). This fits with a suggestion that LCVs might play a more important role in cell-to-cell spreading than SCVs (Coleman et al., 2004). As we only performed morphological analysis, further experiments are required to determine whether the egressed bacteria are LCVs or SCVs.

We can exclude that *C. burnetii* spreading is mediated through formation of membrane protrusions (Figure 4). However, our data suggest that besides programmed cell death induction other forms

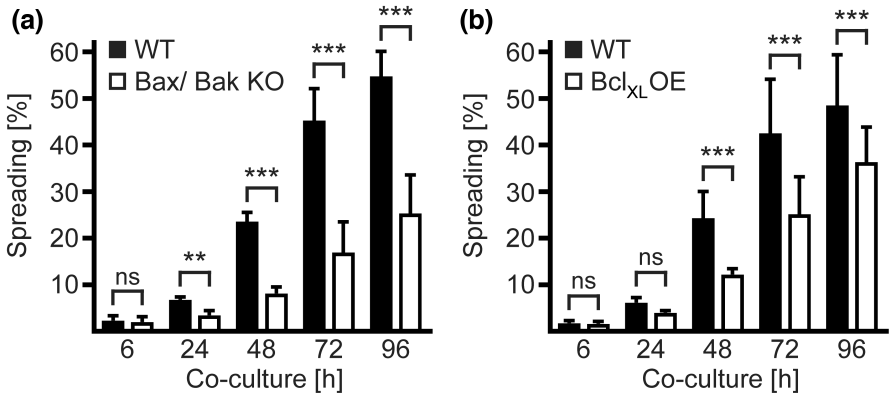

FIGURE 8 Apoptosis of host cells is important for the spread of infection. Bax/Bak double knock-out HeLa cells (Bax/Bak KO, a), Bcl_{XL} overexpressing HeLa cells (Bcl_{XL} OE, b) and their respective control cell lines (WT) were infected with *Coxiella burnetii* TagRFP at a MOI of 200 for 5 days and pre-incubated with 200 μg/mL gentamicin for 4 h. Uninfected HeLa cells were labeled with CellTrace Blue (CTB). The cells were grown together at a ratio of 1:2 (infected: uninfected) for the indicated time periods and 30.000 single cells were analyzed by flow cytometry (BD LSRFortessa) for each sample. Data represent mean percentage ± SD of RFP- and CTB-positive cells out of total CTB-positive cells from three independent experiments in duplicates. ns > 0.05, $^{**}p < 0.01$; $^{***}p < 0.001$.

of the aforementioned egress strategies are exploited by *C. burnetii*. Indeed, we observed exocytosis of *C. burnetii* without host cell lysis (Figure 2b). *C. burnetii* is not an exception, as other pathogens often use more than one egress strategy (Di Venanzio et al., 2017). Therefore, this study can only serve as a starting point to address several open questions regarding the trigger(s), mechanism(s), and mode(s) of *C. burnetii* egress and spreading. More effort is necessary to decipher (i) the role of exocytosis for egress; (ii) the contribution of apoptosis-induction versus exocytosis in egress; (iii) the role of fission of the CCV in egress; (iv) whether egress strategies differ between different host cells, and (v) the role of T4BSS in egress. Our attempts to determine the latter were inconclusive. We detected in preliminary experiments that Δ*dotA* (T4BSS-defective mutant) *C. burnetii* was unable to spread (data not shown). However, the mutant is unable to replicate intracellular (Beare, Gilk, et al., 2011; Carey et al., 2011), resulting in a marked difference in the bacterial load in cells infected with wild-type and Δ*dotA C. burnetii*. Although we tried to compensate for the lack of intracellular replication of the mutant by increasing the infection dose ten-fold, the bacterial load was still lower than in cells infected with wild-type *C. burnetii*. As our data (Figure 5) indicates that the bacterial load is decisive for egress, this might explain the lack of egress of the Δ*dotA* mutant. Thus, further experiments are inevitable to determine the role of the T4BSS in *C. burnetii* egress. In addition, it will be essential to study egress of *C. burnetii* also from alveolar macrophages, which are the first target cells during infection.

4 | EXPERIMENTAL PROCEDURES

4.1 | Reagents

Unless stated otherwise, reagents were purchased from Sigma-Aldrich, Carl Roth, or Thermo Fisher. The LAMP2 (ABL-93) specific primary antibody was developed by J.T. August and obtained from the Developmental Studies Hybridoma Bank, University of Iowa, Department of Biology, Iowa City, IA, USA. Secondary antibodies conjugated with Alexa Fluor-488 or -594 were from Dianova.

4.2 | Cell lines and culture

EA.hy926 (human umbilical vein endothelial cells), HeLa (human epithelial cervix cells) Bax/Bak double knock-out, HeLa Bcl_{XL} overexpression and the corresponding wild-type control cells were all cultured at 37°C and 5% CO_2 in Dulbecco's modified Eagle's medium (Invitrogen) containing either 5% (for infection) or 10% heat-inactivated fetal bovine serum (Biochrom).

FIGURE 9 Intrinsic apoptosis is important for egress of viable *Coxiella burnetii*. Bax/Bak double knock-out HeLa cells (Bax/Bak KO), Bcl_{XL} overexpressing HeLa cells (Bcl_{XL} OE), and their respective control cell lines (WT) were infected with *C. burnetii* TagRFP at a MOI of 200 for 5 days and pre-incubated with 200 μg/mL gentamicin for 4 h. The cells were either left untreated (Mock or -) or incubated with 0.1 μM staurosporine (Stauro) for 4 h (a, b) or 8 h (c). (a) Representative immunofluorescence images after staining for LAMP-1 (green, also surrounding the CCV), for *C. burnetii* (red), and DAPI (blue) are shown. Scale bars are 20 μM. (b) Fragmented nuclei were counted for 100 infected cells each from three independent experiments in duplicate. (c) Egressed viable *C. burnetii* in the supernatants of 6-well plates were determined via counting of colony forming units (CFU). The experiment was performed twice with technical triplicates. (b, c) Error bars indicate ± SD. ns > 0.05, $^{***}p < 0.001$.

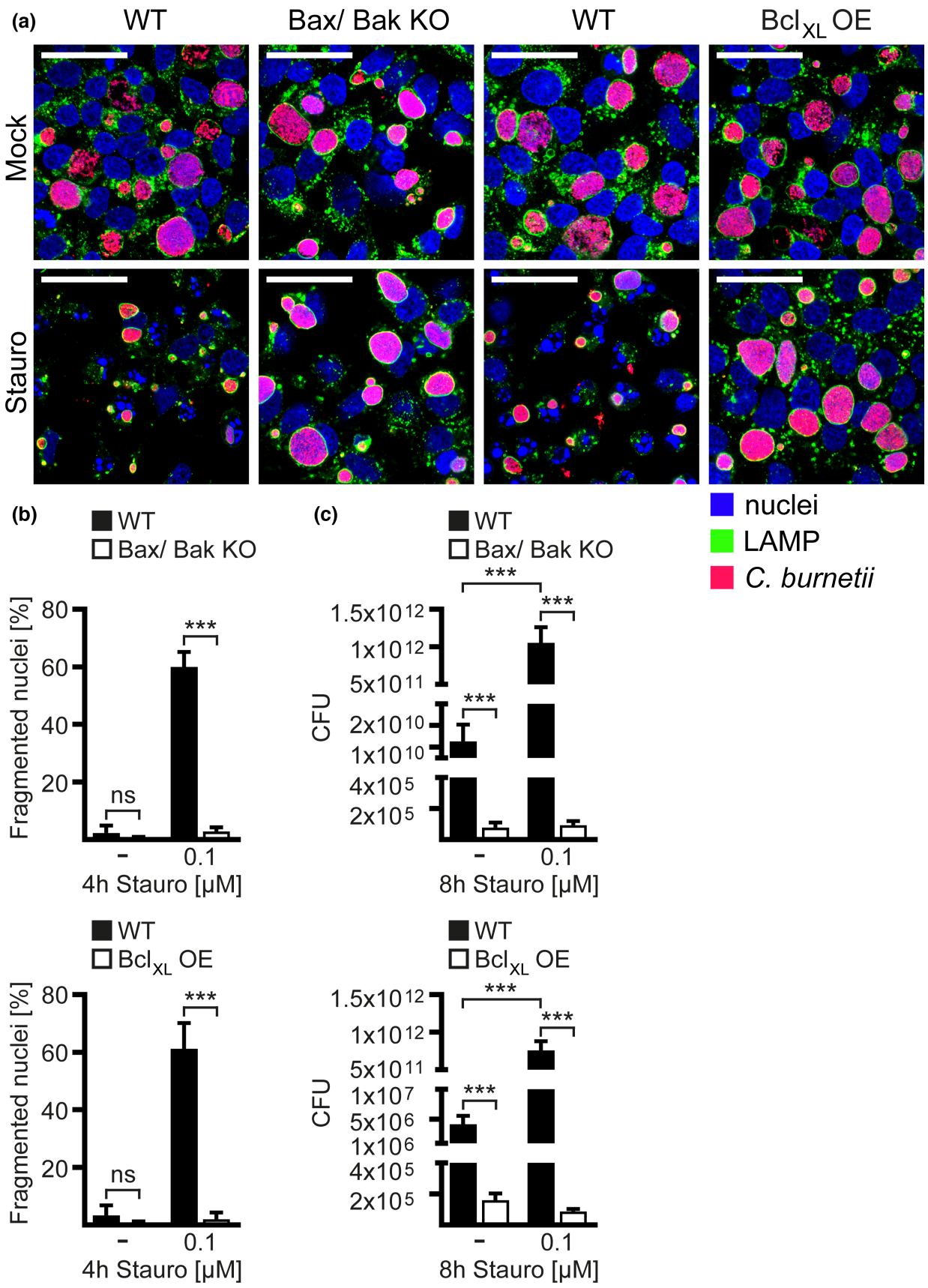

4.3 | Bacterial constructs, strains, and growth conditions

Throughout the study, the *Coxiella burnetii* strain Nine Mile RSA439 phase II was used. *C. burnetii* wild-type GFP (*Tn1832*) and Δ*dotA* GFP-tagged (*Tn514*) transposon mutants were a generous gift of M. Bonazzi (CNRS, University of Montpellier, France) (Martinez et al., 2014, 2015). The plasmid pITR-P1169-Kan-mCherry was kindly provided by Robert Heinzen (Rocky Mountain Laboratories, NIH, Montana, USA) (Beare, Gilk, et al., 2011). For cloning of the IPTG-inducible and chloramphenicol resistant expression construct pKM244mod-TagRFP-c, the TaqRFP encoding gene was amplified by PCR from pTagRFP-c (Merzlyak et al., 2007) using the specific primer set 5´-ACTGACGAATTCAAGGGGAATAGCATA TGGTGTCTAAGGGCGAAGAG and 3´-GCAAGTGGTACCGTTAAT TAAGTTTGTGCCCCAGTTTG, restricted with *Eco*RI and *Kpn*I (underlined in the respective oligonucleotide sequence), and ligated with likewise-restricted pKM244mod (Schäfer et al., 2017). *C. burnetii* were electroporated with 15 μg pITR-P1169-Kan-mCherry or pKM244mod-TagRFP-c as previously described (Beare, Sandoz, et al., 2011). Positive clones were selected with 500 μg/mL kanamycin or 3 μg/mL chloramphenicol, respectively. ACCM-2 medium (Sunrise Science Products) without or with the respective antibiotics was inoculated with 1×10^6/mL of the respective *C. burnetii* strain and incubated at 37°C, 2.5% O_2 and 5% CO_2 for 5 days before infection.

4.4 | *C. burnetii* infection of cell lines

EA.hy926 or HeLa cells were seeded on coverslips in a 24-well plate (1 mL, 5×10^4) for immunofluorescence or in T75 cell culture flasks (15 mL, 2×10^6) for the co-culture, trans-well and spreading assays on the day before infection. To infect cell lines, bacteria grown for 5 days were pelleted and adjusted spectrophotometrically in PBS to yield the respective MOI. Cells were infected by changing the media to DMEM/5% FCS (0.5 mL for 24-well plates and 8 mL for T75 flasks) with the appropriate amount of *C. burnetii*. After 8 h incubation at 37°C, 5% CO_2 the medium was replaced by fresh medium (1.5 mL for 24-well and 15 mL for T75 flask).

4.5 | Apoptosis analysis of *C. burnetii* infected cells with Annexin V staining

HeLa cells, either uninfected or infected at MOI 200 with GFP-tagged *C. burnetii* for 2 or 7 days, were either not treated or treated with 0.1 μM staurosporine for 4 h at 37°C in 5% CO_2. The cells were harvested with trypsin–EDTA, washed with PBS, and 3×10^5 cells were stained with annexin V-phycoerythrin (PE) and 7-aminoactinomycin D (7-AAD) for 15 min in the dark according to the manufacturer's protocol (PE Annexin V apoptosis detection kit I; BD Biosciences). For the gating strategy we utilized the forward and sideward scatter to select the cell population and excluded doublets. For the infected cells we gated additionally on GFP-positive cells. Finally, we obtained the data in a PE vs. 7-AAD dot plot. The percentage of early apoptotic cells (PE-positive and 7-AAD negative) was determined by flow cytometry using a FACS Fortessa (Becton Dickinson), and the data were evaluated with FlowJo software (BD Biosciences).

4.6 | Apoptosis analysis of *C. burnetii* infected cells by PARP cleavage

HeLa cells, either uninfected or infected at MOI 200 with GFP-tagged *C. burnetii* for 2 or 7 days, were either not treated or treated with 0.1 μM staurosporine for 4 h. Proteins of 5×10^5 HeLa cells were separated by SDS-PAGE on a Bolt Bis-Tris Plus 4%–12% gradient gel (Thermo Fisher Scientific) at 160 V for 45 min and transferred to a PVDF membrane (Millipore). For detection of expressed proteins specific primary antibodies against cleaved PARP (Cell Signaling), GFP (Roche), and actin (Sigma) together with corresponding HRP-coupled secondary antibodies (Dianova) were utilized. For visualization by a chemiluminescence detection system (Millipore), a Vilber Fusion FX system (Vilber) with Evolution-Capt software was used.

4.7 | Co-culture experiment

EA.hy926 cells, infected for 4 days with *C. burnetii* TagRFP were seeded on coverslips in a 24-well plate (5×10^4). 16–20 h prior to co-culture, the medium was exchanged to DMEM/10% FCS/2 mM IPTG to induce expression of TagRFP. Uninfected EA.hy926 cells were adjusted to 1×10^6 mL^{-1} in PBS and stained with the CellTrace CFSE Cell Proliferation kit (Thermo Fisher) according to the manufacturer's protocol for 45 min with 5 μM CFSE. For the co-culture assay, 1×10^5 of the uninfected CFSE-labeled EA.hy926 cells were added in DMEM/10% FCS/2 mM IPTG to the 5-day infected EA.hy926 cells on coverslip. After the indicated times of co-culture at 37°C, 5% CO_2, the coverslips were subjected to immunofluorescence analysis.

4.8 | Trans-well assay

EA.hy926 cells (5×10^4), infected for 3 days with *C. burnetii* TagRFP-infected were seeded in the upper chamber of a trans-well chamber with a 3 μm pore size in DMEM/10% FCS/2 mM IPTG to induce expression of TagRFP. After 2 days incubation at 37°C, 5% CO_2 the infected cells formed a confluent layer. Uninfected EA.hy926 cells were adjusted to 1×10^6 mL^{-1} in PBS and stained with the CellTrace CFSE Cell Proliferation kit (Thermo Fisher) according to the manufacturer's protocol for 45 min with 5 μM CFSE. 5×10^4 of the uninfected CFSE-labeled EA.hy926 cells were

seeded in DMEM/10% FCS on a coverslip for 24 h. The cells were washed three times with PBS. The washed upper chamber with a confluent monolayer of cells infected for 5 days was placed above the coverslip with the uninfected cells in the lower chamber in DMEM/10% FCS/2 mM IPTG. After the indicated times of incubation at 37°C, 5% CO_2, the coverslips were subjected to immunofluorescence analysis.

4.9 | FACS-based spreading assay

EA.hy926 or Hela cells, infected with GFP- or TagRFP-expressing *C. burnetii* for 4 days were seeded in six-well plates (2 mL, 1×10^5). 20 h post seeding, cells were washed twice with PBS, before new medium containing 200 μg/mL^{-1} gentamicin was added for 4 h at 37°C, 5% CO_2. Uninfected cells of the same cell line were adjusted to 1×10^6 mL^{-1} in PBS and stained with CellTrace Blue (CTB) according to the manufacturer's protocol (5 μM, 1 h). After washing off gentamicin, 3×10^5 uninfected CTB-labeled cells were added to the infected cells in 3 mL DMEM, 10% FCS, and 2 mM IPTG. After co-incubation at 37°C, 5% CO_2, the cells were detached from the plate fat the time points indicated using trypsin/EDTA and resuspended in 500 μL PBS before being counted with a BD LSRFortessa Flow cytometer. Single, living cells were gated by FSC-A/SSC-A and SSC-A/SSC-H and analyzed for GFP (488 nm laser; 505LP, 530/30BP filter set) or TagRFP (561 nm laser; 586/15BP filter) together with CellTrace Blue (355 nm laser; 390/18BP filter). Spreading was calculated as mean percentage of RFP- or GFP- and CTB-positive cells out of the total number of CTB-positive cells.

4.10 | Indirect immunofluorescence and live cell imaging

Infected EA.hy926 or HeLa cells on coverslips in a 24-well plate were fixed with 4% paraformaldehyde (Alfa Aesar) in PBS (Biochrom) for 15 min at room temperature in the dark, permeabilized with ice-cold methanol for 1 min, quenched with 50 mM NH_4Cl (Roth) in blocking buffer (PBS with 5% goat serum; Life Technologies) for 30 min at room temperature. The coverslips were incubated for 2 h with anti-LAMP2 (DSHB) and anti-*C. burnetii* in blocking buffer, washed three times with PBS, and incubated with secondary Alexa Fluor labeled antibodies Alexa 488 and Alexa 594 (Dianova) for 30 min in blocking buffer at room temperature. The cells were mounted using ProLong Diamond with DAPI (Thermo Fisher). For the co-culture and trans-well assay experiments, specimens were mounted directly after fixation and permeabilization. Analysis was performed using the Carl Zeiss LSM 700 Laser Scanning Confocal Microscope, recording data with a 63x/1.4 oil immersion objective lens and Zen software (Carl Zeiss, Oberkochen, Germany).

For live cell imaging, EA.hy926 infected for 4 days with *C. burnetii* mCherry were seeded in a 35 mm glass bottom dish No 1.0 (MatTek, 2×10^5) in 2 mL DMEM, 10% FCS and 2 mM IPTG. Twenty-four hours post-seeding SiR actin (Spirochrome) was added at 50 nmol in new cell culture media with IPTG and different regions of infected cells were visualized every 15 min for 12 h with a Zeiss Spinning Disc Axio Observer Z1 (Carl Zeiss, Oberkochen, Germany).

4.11 | Transmission electron microscopy

EA.hy926 cells grown in two 10 cm-culture dishes were inoculated with a 200 MOI of *C. burnetii* NMII. After 7 days, the medium was removed and the cells were fixed with 2.5% glutaraldehyde in 0.1 M cacodylate buffer (pH 7.2) containing 1.8% glucose for 8 h at 4°C. Then, the fixative was replaced by cacodylate buffer. The cells were gently scraped off the dishes, collected in an Eppendorf tube, and centrifuged for 5 min at 1500 × g in an Eppendorf centrifuge to obtain a pellet. EA.hy926 cells grown in three T175 cell culture flasks were infected as described above. After 10 days, the culture supernatant was collected, and centrifuged at 138 x g for 5 min, then the supernatant at 4500 × g for 20 min to obtain a pellet. After fixation with 2.5% glutaraldehyde in 0.1 M cacodylate buffer (pH 7.2) containing 1.8% glucose for 8 h at 4°C, the fixative was replaced by cacodylate buffer. For resin embedding, the pellets were evenly mixed with 20 μL of 2% molten agarose on a glass slide, allowed to cool, and sectioned into 1 mm^3 cubes. Cubes were post-fixed in 2% osmium tetroxide and embedded in Araldite Cy212. Relevant areas were selected in Toluidine-blue-stained semi-thin sections. Ultrathin sections (85 nm) collected on 200 mesh copper grids were stained with uranyl acetate and lead citrate and examined by transmission electron microscopy (Tecnai 12; FEI/ThermoFisher Scientific) at 80 kV. Representative electron micrographs were taken using a 4k × 4k digital CMOS camera (TEMCAM FX416, TVIPS, Garching, Germany).

4.12 | Apoptosis analysis of *C. burnetii* infected cells with nuclear fragmentation assay

HeLa Bax/Bak double knock-out, HeLa Bcl_{XL} overexpressing, and the respective wild-type control cells were seeded on coverslips in 24-well plates at a density of 5×10^4. 24 h after plating, the cells were infected with *C. burnetii* at a MOI of 200 and incubated for 5 days. After pre-incubation with 200 μg/mL gentamicin for 4 h at 37°C, 5% CO_2, the cells were either left untreated or were treated with 0.1 μM staurosporine (Cell Signaling) for 4 h. The specimens were prepared for indirect immunofluorescence with antibodies against *C. burnetii* and LAMP2 as described above and mounted using ProLong Diamond with DAPI (Thermo Fisher). The percentage of infected cells with fragmented or condensed nuclei was determined using an

epifluorescense microscope as described previously (Klingenbeck et al., 2013).

4.13 | Colony-forming units (CFU) count of egressed *C. burnetii* from infected cells

HeLa Bax/Bak double knock-out, HeLa Bcl_{XL} overexpressing, and the respective corresponding wild-type control cells were seeded 24 h before infection at a density of 2×10^5 in 6-well plates. They were infected with *C. burnetii* at a MOI of 200 and cultured for 5 days. After pre-incubation with 200 μg/mL gentamicin for 4 h at 37°C, 5% CO_2, the cells were either left untreated or were treated with 0.1 μM staurosporine (Cell Signaling) for 8 h. The supernatants were harvested carefully and the pellets (1 min, 12,000 × g) were resuspended in 200 μL PBS, pH 7.4 each before preparing serial dilutions in ACCM-2. The dilutions were pipetted in triplicates on ACCM-2/0.5 mM tryptophane/0.5% agarose plates, incubated for 10 days at 37°C, 5% CO_2 and 2.5% O_2 before the CFUs were finally counted.

4.14 | Statistical analysis

Statistical analysis was conducted with Prism 8 (GraphPad software). Bar graphs depict mean data ± standard deviation from three independent experiments in duplicates. An unpaired Student's *t*-test was performed to determine the significance of the results, and a *p*-value of <0.05 was considered significant.

AUTHOR CONTRIBUTIONS

Anja Lührmann: Conceptualization; funding acquisition; writing – original draft; writing – review and editing; project administration; supervision; resources. **Jan Schulze-Luehrmann:** Conceptualization; investigation; visualization; validation; formal analysis; writing – review and editing. **Elisabeth Liebler-Tenorio:** Investigation; methodology; visualization; writing – review and editing. **Alfonso Felipe-López:** Visualization; investigation; writing – review and editing.

ACKNOWLEDGEMENTS

This work was supported by the Deutsche Forschungsgemeinschaft (DFG) through the Priority Programme SPP2225 (LU 1357/7-1) to AL and by the Bundesministerium für Bildung und Forschung (BMBF) under the project number 01KI1726A/01KI2008A of "Q-GAPS" as part of the research network zoonotic infectious diseases to AL. We thank Marcus Pfau for photographic work and editing of the EM samples, Lisa Wolf for preparation of the EM samples, Dr. Christian Berens for critically reading the manuscript, and Prof. Dr. Georg Häcker for providing the HeLa Bax/Bak knock-out and HeLa Bcl_{XL} overexpression cell lines. Open Access funding enabled and organized by Projekt DEAL.

CONFLICT OF INTEREST STATEMENT

The authors declare that the research was conducted in the absence of any commercial or financial relationships that could be construed as a potential conflict of interest.

DATA AVAILABILITY STATEMENT

The data that support the findings of this study are available from the corresponding author upon reasonable request.

ETHICS STATEMENT

Not applicable for this study.

ORCID

Anja Lührmann https://orcid.org/0000-0003-1224-0880

REFERENCES

Anderson, A., Bijlmer, H., Fournier, P.E., Graves, S., Hartzell, J., Kersh, G.J. et al. (2013) Diagnosis and management of Q fever—United States, 2013: recommendations from CDC and the Q Fever Working Group. *MMWR. Recommendations and Reports: Morbidity and Mortality Weekly Report. Recommendations and Reports*, 62, 1–30.

Angelakis, E. & Raoult, D. (2010) Q fever. *Veterinary Microbiology*, 140, 297–309.

Atzpodien, E., Baumgartner, W., Artelt, A. & Thiele, D. (1994) Valvular endocarditis occurs as a part of a disseminated *Coxiella burnetii* infection in immunocompromised BALB/cJ (H-2d) mice infected with the nine mile isolate of *C. burnetii*. *The Journal of Infectious Diseases*, 170, 223–226.

Baca, O.G., Scott, T.O., Akporiaye, E.T., DeBlassie, R. & Crissman, H.A. (1985) Cell cycle distribution patterns and generation times of L929 fibroblast cells persistently infected with *Coxiella burnetii*. *Infection and Immunity*, 47, 366–369.

Beare, P.A., Gilk, S.D., Larson, C.L., Hill, J., Stead, C.M., Omsland, A. et al. (2011) Dot/Icm type IVB secretion system requirements for *Coxiella burnetii* growth in human macrophages. *MBio*, 2, e00175-11.

Beare, P.A., Sandoz, K.M., Omsland, A., Rockey, D.D. & Heinzen, R.A. (2011) Advances in genetic manipulation of obligate intracellular bacterial pathogens. *Frontiers in Microbiology*, 2, 97.

Bertheloot, D., Latz, E. & Franklin, B.S. (2021) Necroptosis, pyroptosis and apoptosis: an intricate game of cell death. *Cellular & Molecular Immunology*, 18, 1106–1121.

Bisle, S., Klingenbeck, L., Borges, V., Sobotta, K., Schulze-Luehrmann, J., Menge, C. et al. (2016) The inhibition of the apoptosis pathway by the *Coxiella burnetii* effector protein CaeA requires the EK repetition motif, but is independent of Survivin. *Virulence*, 7, 400–412.

Briggs, H.L., Pul, N., Seshadri, R., Wilson, M.J., Tersteeg, C., Russell-Lodrigue, K.E. et al. (2008) Limited role for iron regulation in *Coxiella burnetii* pathogenesis. *Infection and Immunity*, 76, 2189–2201.

Brokatzky, D., Dorflinger, B., Haimovici, A., Weber, A., Kirschnek, S., Vier, J. et al. (2019) A non-death function of the mitochondrial apoptosis apparatus in immunity. *The EMBO Journal*, 38, e100907.

Brokatzky, D., Kretz, O. & Hacker, G. (2020) Apoptosis functions in defense against infection of mammalian cells with environmental Chlamydiae. *Infection and Immunity*, 88, e00851-19.

Burette, M., Allombert, J., Lambou, K., Maarifi, G., Nisole, S., Di Russo Case, E. et al. (2020) Modulation of innate immune signaling by a *Coxiella burnetii* eukaryotic-like effector protein. *Proceedings of the National Academy of Sciences of the United States of America*, 117, 13708–13718.

Campoy, E.M., Zoppino, F.C. & Colombo, M.I. (2011) The early secretory pathway contributes to the growth of the *Coxiella*-replicative niche. *Infection and Immunity*, 79, 402–413.

Capo, C., Lindberg, F.P., Meconi, S., Zaffran, Y., Tardei, G., Brown, E.J. et al. (1999) Subversion of monocyte functions by *Coxiella burnetii*: impairment of the cross-talk between alphavbeta3 integrin and CR3. *Journal of Immunology*, 163, 6078–6085.

Carey, K.L., Newton, H.J., Lührmann, A. & Roy, C.R. (2011) The *Coxiella burnetii* dot/Icm system delivers a unique repertoire of type IV effectors into host cells and is required for intracellular replication. *PLoS Pathogens*, 7, e1002056.

Chen, C., Banga, S., Mertens, K., Weber, M.M., Gorbaslieva, I., Tan, Y. et al. (2010) Large-scale identification and translocation of type IV secretion substrates by *Coxiella burnetii*. *Proceedings of the National Academy of Sciences of the United States of America*, 107, 21755–21760.

Coleman, S.A., Fischer, E.R., Howe, D., Mead, D.J. & Heinzen, R.A. (2004) Temporal analysis of *Coxiella burnetii* morphological differentiation. *Journal of Bacteriology*, 186, 7344–7352.

Cordsmeier, A., Rinkel, S., Jeninga, M., Schulze-Luehrmann, J., Olke, M., Schmid, B. et al. (2022) The *Coxiella burnetii* T4SS effector protein AnkG hijacks the 7SK small nuclear ribonucleoprotein complex for reprogramming host cell transcription. *PLoS Pathogens*, 18, e1010266.

Cordsmeier, A., Wagner, N., Lührmann, A. & Berens, C. (2019) Defying death - how *Coxiella burnetii* copes with intentional host cell suicide. *The Yale Journal of Biology and Medicine*, 92, 619–628.

Cunha, L.D., Ribeiro, J.M., Fernandes, T.D., Massis, L.M., Khoo, C.A., Moffatt, J.H. et al. (2015) Inhibition of inflammasome activation by *Coxiella burnetii* type IV secretion system effector IcaA. *Nature Communications*, 6, 10205.

Dellacasagrande, J., Ghigo, E., Hammami, S.M., Toman, R., Raoult, D., Capo, C. et al. (2000) Alpha(v)beta(3) integrin and bacterial lipopolysaccharide are involved in *Coxiella burnetii*-stimulated production of tumor necrosis factor by human monocytes. *Infection and Immunity*, 68, 5673–5678.

Delsing, C.E., Warris, A. & Bleeker-Rovers, C.P. (2011) Q fever: still more queries than answers. *Advances in Experimental Medicine and Biology*, 719, 133–143.

Di Venanzio, G., Lazzaro, M., Morales, E.S., Krapf, D. & Garcia Vescovi, E. (2017) A pore-forming toxin enables Serratia a nonlytic egress from host cells. *Cellular Microbiology*, 19, e12656.

Eckart, R.A., Bisle, S., Schulze-Luehrmann, J., Wittmann, I., Jantsch, J., Schmid, B. et al. (2014) Antiapoptotic activity of *Coxiella burnetii* effector protein AnkG is controlled by p32-dependent trafficking. *Infection and Immunity*, 82, 2763–2771.

Eldin, C., Melenotte, C., Mediannikov, O., Ghigo, E., Million, M., Edouard, S. et al. (2017) From Q fever to *Coxiella burnetii* infection: a paradigm change. *Clinical Microbiology Reviews*, 30, 115–190.

Fielden, L.F., Moffatt, J.H., Kang, Y., Baker, M.J., Khoo, C.A., Roy, C.R. et al. (2017) A Farnesylated *Coxiella burnetii* effector forms a Multimeric complex at the mitochondrial outer membrane during infection. *Infection and Immunity*, 85, 85.

Fielden, L.F., Scott, N.E., Palmer, C.S., Khoo, C.A., Newton, H.J. & Stojanovski, D. (2021) Proteomic identification of *Coxiella burnetii* effector proteins targeted to the host cell mitochondria during infection. *Molecular & Cellular Proteomics*, 20, 100005.

Flieger, A., Frischknecht, F., Hacker, G., Hornef, M.W. & Pradel, G. (2018) Pathways of host cell exit by intracellular pathogens. *Microbial cell*, 5, 525–544.

Friedrich, A., Pechstein, J., Berens, C. & Lührmann, A. (2017) Modulation of host cell apoptotic pathways by intracellular pathogens. *Current Opinion in Microbiology*, 35, 88–99.

Friedrich, N., Hagedorn, M., Soldati-Favre, D. & Soldati, T. (2012) Prison break: Pathogens' strategies to egress from host cells. *Microbiology and Molecular Biology Reviews*, 76, 707–720.

Gutierrez, M.G., Vazquez, C.L., Munafo, D.B., Zoppino, F.C., Beron, W., Rabinovitch, M. et al. (2005) Autophagy induction favours the generation and maturation of the *Coxiella*-replicative vacuoles. *Cellular Microbiology*, 7, 981–993.

Howe, D. & Mallavia, L.P. (1999) *Coxiella burnetii* infection increases transferrin receptors on J774A.1 cells. *Infection and Immunity*, 67, 3236–3241.

Howe, D., Melnicakova, J., Barak, I. & Heinzen, R.A. (2003) Maturation of the *Coxiella burnetii* parasitophorous vacuole requires bacterial protein synthesis but not replication. *Cellular Microbiology*, 5, 469–480.

Howe, D., Shannon, J.G., Winfree, S., Dorward, D.W. & Heinzen, R.A. (2010) *Coxiella burnetii* phase I and II variants replicate with similar kinetics in degradative phagolysosome-like compartments of human macrophages. *Infection and Immunity*, 78, 3465–3474.

Kersh, G.J. (2013) Antimicrobial therapies for Q fever. *Expert Review of Anti-Infective Therapy*, 11, 1207–1214.

Klingenbeck, L., Eckart, R.A., Berens, C. & Lührmann, A. (2013) The *Coxiella burnetii* type IV secretion system substrate CaeB inhibits intrinsic apoptosis at the mitochondrial level. *Cellular Microbiology*, 15, 675–687.

Koch, R.D., Horner, E.M., Munch, N., Maier, E. & Kozjak-Pavlovic, V. (2020) Modulation of host cell death and lysis are required for the release of *Simkania negevensis*. *Frontiers in Cellular and Infection Microbiology*, 10, 594932.

Kohler, L.J., Reed, S.R., Sarraf, S.A., Arteaga, D.D., Newton, H.J. & Roy, C.R. (2016) Effector protein Cig2 decreases host tolerance of infection by directing constitutive fusion of autophagosomes with the *Coxiella*-containing vacuole. *MBio*, 7, e01127-16.

Larson, C.L., Beare, P.A., Howe, D. & Heinzen, R.A. (2013) *Coxiella burnetii* effector protein subverts clathrin-mediated vesicular trafficking for pathogen vacuole biogenesis. *Proceedings of the National Academy of Sciences of the United States of America*, 110, E4770–E4779.

Larson, C.L., Beare, P.A., Voth, D.E., Howe, D., Cockrell, D.C., Bastidas, R.J. et al. (2015) *Coxiella burnetii* effector proteins that localize to the parasitophorous vacuole membrane promote intracellular replication. *Infection and Immunity*, 83, 661–670.

Larson, C.L., Martinez, E., Beare, P.A., Jeffrey, B., Heinzen, R.A. & Bonazzi, M. (2016) Right on Q: genetics begin to unravel *Coxiella burnetii* host cell interactions. *Future Microbiology*, 11, 919–939.

Latomanski, E.A., Newton, P., Khoo, C.A. & Newton, H.J. (2016) The effector Cig57 hijacks FCHO-mediated vesicular trafficking to facilitate intracellular replication of *Coxiella burnetii*. *PLoS Pathogens*, 12, e1006101.

Lührmann, A., Newton, H.J. & Bonazzi, M. (2017) Beginning to understand the role of the type IV secretion system effector proteins in *Coxiella burnetii* pathogenesis. *Current Topics in Microbiology and Immunology*, 413, 243–268.

Lührmann, A., Nogueira, C.V., Carey, K.L. & Roy, C.R. (2010) Inhibition of pathogen-induced apoptosis by a *Coxiella burnetii* type IV effector protein. *Proceedings of the National Academy of Sciences of the United States of America*, 107, 18997–19001.

Lührmann, A. & Roy, C.R. (2007) *Coxiella burnetii* inhibits activation of host cell apoptosis through a mechanism that involves preventing cytochrome c release from mitochondria. *Infection and Immunity*, 75, 5282–5289.

Martinez, E., Allombert, J., Cantet, F., Lakhani, A., Yandrapalli, N., Neyret, A. et al. (2016) *Coxiella burnetii* effector CvpB modulates phosphoinositide metabolism for optimal vacuole development. *Proceedings of the National Academy of Sciences of the United States of America*, 113, E3260–E3269.

Martinez, E., Cantet, F. & Bonazzi, M. (2015) Generation and multiphenotypic high-content screening of *Coxiella burnetii* transposon mutants. *Journal of Visualized Experiments: JoVE*, 99, e52851.

Martinez, E., Cantet, F., Fava, L., Norville, I. & Bonazzi, M. (2014) Identification of OmpA, a *Coxiella burnetii* protein involved in host

cell invasion, by multi-phenotypic high-content screening. *PLoS Pathogens*, 10, e1004013.
Maurin, M. & Raoult, D. (1999) Q fever. *Clinical Microbiology Reviews*, 12, 518–553.
Merzlyak, E.M., Goedhart, J., Shcherbo, D., Bulina, M.E., Shcheglov, A.S., Fradkov, A.F. et al. (2007) Bright monomeric red fluorescent protein with an extended fluorescence lifetime. *Nature Methods*, 4, 555–557.
Moormeier, D.E., Sandoz, K.M., Beare, P.A., Sturdevant, D.E., Nair, V., Cockrell, D.C. et al. (2019) *Coxiella burnetii* RpoS regulates genes involved in morphological differentiation and intracellular growth. *Journal of Bacteriology*, 201, e00009-19.
Morroy, G., Keijmel, S.P., Delsing, C.E., Bleijenberg, G., Langendam, M., Timen, A. et al. (2016) Fatigue following acute Q-fever: a systematic literature review. *PLoS One*, 11, e0155884.
Newton, H.J., McDonough, J.A. & Roy, C.R. (2013) Effector protein translocation by the *Coxiella burnetii* Dot/Icm type IV secretion system requires endocytic maturation of the pathogen-occupied vacuole. *PLoS One*, 8, e54566.
O'Connor, T.J., Zheng, H., VanRheenen, S.M., Ghosh, S., Cianciotto, N.P. & Isberg, R.R. (2016) Iron limitation triggers early egress by the intracellular bacterial pathogen *Legionella pneumophila*. *Infection and Immunity*, 84, 2185–2197.
Sanchez, S.E. & Omsland, A. (2020) Critical role for molecular iron in *Coxiella burnetii* replication and viability. *mSphere*, 5, e00458-20.
Sandoz, K.M., Beare, P.A., Cockrell, D.C. & Heinzen, R.A. (2016) Complementation of arginine Auxotrophy for genetic transformation of *Coxiella burnetii* by use of a defined axenic medium. *Applied and Environmental Microbiology*, 82, 3042–3051.
Schäfer, W., Eckart, R.A., Schmid, B., Cagköylü, H., Hof, K., Muller, Y.A. et al. (2017) Nuclear trafficking of the anti-apoptotic *Coxiella burnetii* effector protein AnkG requires binding to p32 and importin-alpha1. *Cellular Microbiology*, 19, e12634.
Schäfer, W., Schmidt, T., Cordsmeier, A., Borges, V., Beare, P.A., Pechstein, J. et al. (2020) The anti-apoptotic *Coxiella burnetii* effector protein AnkG is a strain specific virulence factor. *Scientific Reports*, 10, 15396.
Schulze-Luehrmann, J., Eckart, R.A., Ölke, M., Saftig, P., Liebler-Tenorio, E. & Lührmann, A. (2016) LAMP proteins account for the maturation delay during the establishment of the *Coxiella burnetii*-containing vacuole. *Cellular Microbiology*, 18, 181–194.
Traven, A. & Naderer, T. (2014) Microbial egress: a Hitchhiker's guide to freedom. *PLoS Pathogens*, 10, e1004201.
Van den Brom, R., van Engelen, E., Roest, H.I., van der Hoek, W. & Vellema, P. (2015) *Coxiella burnetii* infections in sheep or goats: an opinionated review. *Veterinary Microbiology*, 181, 119–129.
van Schaik, E.J., Chen, C., Mertens, K., Weber, M.M. & Samuel, J.E. (2013) Molecular pathogenesis of the obligate intracellular bacterium *Coxiella burnetii*. *Nature Reviews. Microbiology*, 11, 561–573.
VanCleave, T.T., Pulsifer, A.R., Connor, M.G., Warawa, J.M. & Lawrenz, M.B. (2017) Impact of gentamicin concentration and exposure time on intracellular *Yersinia pestis*. *Frontiers in Cellular and Infection Microbiology*, 7, 505.
Voth, D.E. & Heinzen, R.A. (2007) Lounging in a lysosome: the intracellular lifestyle of *Coxiella burnetii*. *Cellular Microbiology*, 9, 829–840.
Voth, D.E. & Heinzen, R.A. (2009) Sustained activation of Akt and Erk1/2 is required for *Coxiella burnetii* antiapoptotic activity. *Infection and Immunity*, 77, 205–213.
Voth, D.E., Howe, D. & Heinzen, R.A. (2007) *Coxiella burnetii* inhibits apoptosis in human THP-1 cells and monkey primary alveolar macrophages. *Infection and Immunity*, 75, 4263–4271.
Weber, M.M., Chen, C., Rowin, K., Mertens, K., Galvan, G., Zhi, H. et al. (2013) Identification of *Coxiella burnetii* type IV secretion substrates required for intracellular replication and Coxiella-containing vacuole formation. *Journal of Bacteriology*, 195, 3914–3924.
Weber, M.M., Faris, R., van Schaik, E.J., McLachlan, J.T., Wright, W.U., Tellez, A. et al. (2016) The type IV secretion system effector protein CirA stimulates the GTPase activity of RhoA and is required for virulence in a mouse model of *Coxiella burnetii* infection. *Infection and Immunity*, 84, 2524–2533.
Weddle, E. & Agaisse, H. (2018) Principles of intracellular bacterial pathogen spread from cell to cell. *PLoS Pathogens*, 14, e1007380.
Zhang, Y., Zhang, G., Hendrix, L.R., Tesh, V.L. & Samuel, J.E. (2012) *Coxiella burnetii* induces apoptosis during early stage infection via a caspase-independent pathway in human monocytic THP-1 cells. *PLoS One*, 7, e30841.

SUPPORTING INFORMATION

Additional supporting information can be found online in the Supporting Information section at the end of this article.

How to cite this article: Schulze-Luehrmann, J., Liebler-Tenorio, E., Felipe-López, A. & Lührmann, A. (2024) Cell death induction facilitates egress of *Coxiella burnetii* from infected host cells at late stages of infection. *Molecular Microbiology*, 121, 513–528. Available from: https://doi.org/10.1111/mmi.15210